Supporting Information

Integrated BiPO4 nanocrystals/BiOBr heterojunction for sensitive photoelectrochemical sensing of 4-chlorophenol

Li Xu[a], Desheng Jiang[a], Yu Zhao[a], Pengcheng Yan[a], Jintao Dong[c], Junchao Qian[b], Huaqin Ao[a], Jiawen Li[a], Cheng Yan[b,*], Henan Li[a,b*]

[a] School of Chemistry and Chemical Engineering; Institute for Energy Research, Jiangsu University, Zhenjiang 212013, P. R. China

[b] School of Chemistry, Physics and Mechanical Engineering, Queensland University of Technology (QUT), Brisbane, QLD 4001, Australia.

[c] Jiangsu Key Laboratory for Environment Functional Materials, School of Environmental Science and Engineering, Suzhou University of Science and Technology, Suzhou 215009, P. R. China

*Corresponding authors:

c2.yan@qut.edu.au (C. Yan)

lhn@ujs.edu.cn (H.N. Li)

According to the similar method (Experimental section), different mass ratios of $BiPO_4$/BiOBr (5 wt% and 10 wt%) heterojunction was obtained, respectively. Furthermore, XRD analysis was used to characterize the crystal structure and phase of the prepared materials. Fig. S1a shows XRD patterns for $BiPO_4$, BiOBr, and $BiPO_4$/BiOBr heterojunction. It can be observed that all diffraction peaks of $BiPO_4$ were consistent with the standard peaks of monoclinic $BiPO_4$ (JCPDS, No., 15-0767)[1]. In XRD patterns of BiOBr, all typical diffraction peaks corresponded to the tetragonal BiOBr standard card (JCPDS, card, No., 09-0393). For $BiPO_4$/BiOBr heterojunction, the diffraction peaks of $BiPO_4$ and BiOBr were both appeared. The high intensity and sharp diffraction peaks indicate that the prepared $BiPO_4$/BiOBr heterojunction possessed a good crystallinity. No diffraction peak of other impurities existed in the XRD patterns, suggesting that $BiPO_4$/BiOBr heterojunction was formed by coupling BiOBr and $BiPO_4$ with single phase.

In order to further analyze the composition of as-prepared materials, the samples were characterized by infrared spectroscopy. Fig. S1b shows the FT-IR spectra of BiOBr, $BiPO_4$, and $BiPO_4$/BiOBr heterojunction. Four typical absorption peaks were located ranging from 925 cm^{-1} to 1100 cm^{-1} in $BiPO_4$/BiOBr heterojunction, ascribing to the stretching vibration of P-O[2]. There were three characteristic peaks at 600 cm^{-1}, 535 cm^{-1}, and 579 cm^{-1}, respectively, corresponding to the flexural vibrations of delta (O-P-O) and O=P-O[3], which was originated from $BiPO_4$ in $BiPO_4$/BiOBr heterojunction. In addition, the characteristic absorption peaks of Bi-O bond originated from BiOBr appeared at 514cm^{-1} in $BiPO_4$/BiOBr heterojunction[4]. In a word, the typical absorption peaks of BiOBr and $BiPO_4$ were observed in the $BiPO_4$/BiOBr heterojunction. The results of FT-IR suggest that $BiPO_4$/BiOBr heterojunction was successfully prepared.

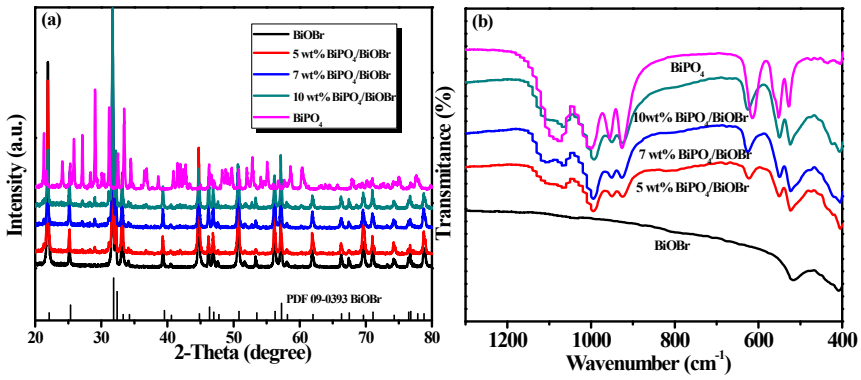

Fig. S1. XRD patterns (a) and FT-IR patterns (b) of BiOBr, $BiPO_4$ and all $BiPO_4$/BiOBr heterojunction with different $BiPO_4$ contents.

The band gap energy (Eg) of the BiOBr and $BiPO_4$ was calculated according to the formula: $\alpha h\nu = A(h\nu - Eg)^{n/2}$, respectively, where α, h, ν, and A stand for the absorption coefficient, Planck constant, light frequency, and a constant[5]. In addition, the n in the equation was depended on the characteristics of the transition in a semiconductor (n = 1 for direct transition and n = 4 for indirect transition). As previous literature reported, the n value of $BiPO_4$ and BiOBr was both 4[6]. The Eg of $BiPO_4$ and BiOBr was estimated to be 3.5 and 2.90 eV, respectively, from the plot of $(\alpha h\nu)^2$ versus (hν) in Fig. S2b, which were close to those in some reported literatures[6].

The photocurrent response of BiOBr/ITO, $BiPO_4$/ITO and $BiPO_4$/BiOBr/ITO was tested by repeated 10 times for 20 seconds at the potential of 0 V, respectively. As shown in Fig. S3, all $BiPO_4$/BiOBr/ITO electrodes showed increased photocurrent, compared with BiOBr/ITO and $BiPO_4$/ITO. The photocurrent of all electrodes did not change significantly after repeated irradiation. It shows that BiOBr/ITO, $BiPO_4$/ITO and all $BiPO_4$/BiOBr/ITO were relatively stable and suitable for constructing photoelectrochemical detection platform. The 7 wt% $BiPO_4$/BiOBr/ITO exhibited the highest transient photocurrent response capability. Therefore, 7 wt% $BiPO_4$/BiOBr/ITO electrode was used to construct PEC sensor.

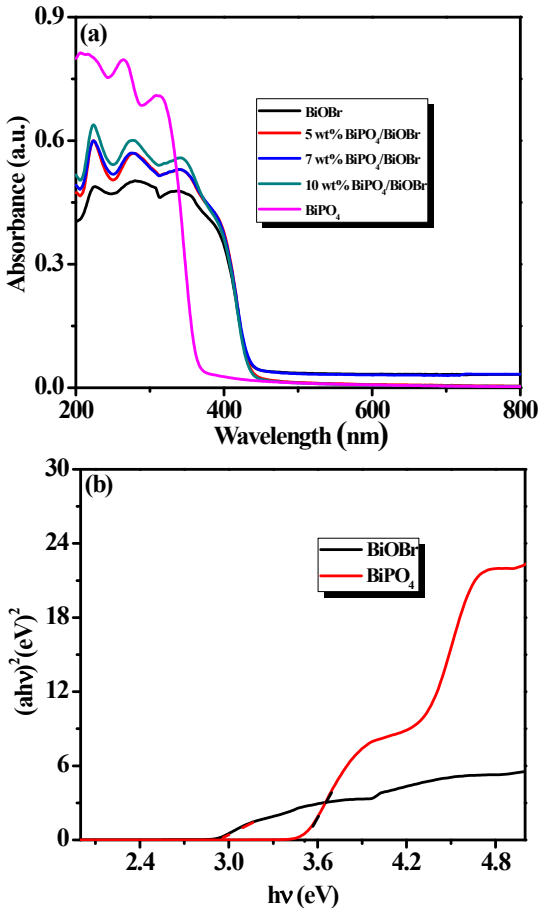

Fig. S2. (a) UV-vis diffused reflectance spectra of $BiPO_4$/BiOBr heterojunction, $BiPO_4$ and BiOBr; (b) The band gap energy of $BiPO_4$ and BiOBr.

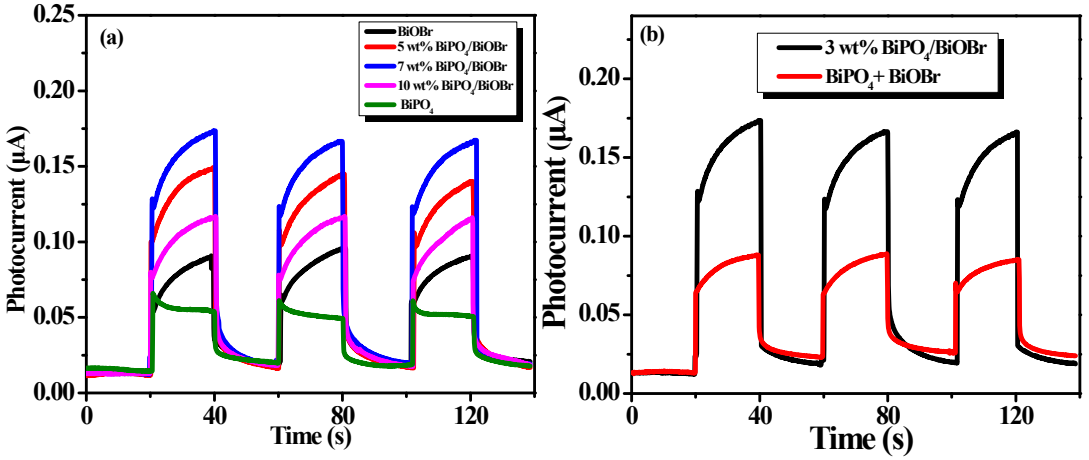

Fig. S3 (a) Transient photocurrent response for BiOBr, $BiPO_4$ and all $BiPO_4$/BiOBr heterojunction; (b) Transient photocurrent response for 3 wt% $BiPO_4$/BiOBr heterojunction and physical mixture of $BiPO_4$ and BiOBr at the same weight percent ratio.

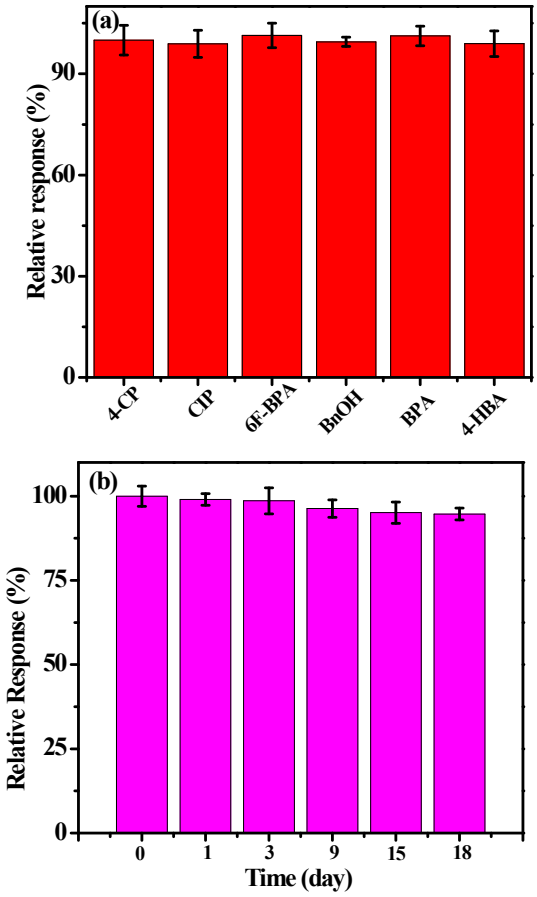

Fig. S4. (a) Influence of particular possible interfering substances on the responses of the photoelectrochemical sensor for 4-CP (80 ng mL^{-1}) in phosphate buffer solution (0.1 M, pH 7.0); (b) Stability tests of photoelectrochemical sensor for detection of 4-CP (80 ng mL^{-1}).

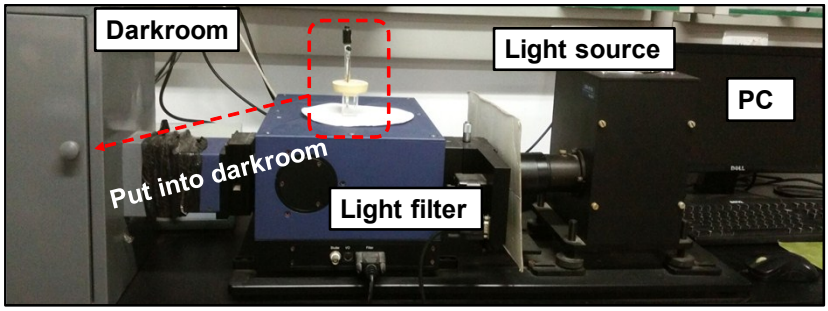

Figure S5. Photograph of PEC detection system.

Tab. S1 Comparison of proposed sensor with other previously reported sensors for 4-CP determination.

Detection method	Linear range (ng mL^{-1})	Detection limit (ng mL^{-1})	Reference
Differential pulse voltammetric detection	1.03×10^2-1.29×10^5	38.57	7
Voltammetric detection	38.56-5.14×10^5	14.14	8
Differential pulse voltammetric detection	1.28×10^4-3.85×10^5	4.74×10^2	9
Amperometric detection	3.21×10^2-5.14×10^3; 8.04×10^3-1.51×10^4	50.13	10
Photoelectrochemical detection	8-2.40×10^3	3.75	This work

Tab. S2. PEC detection of 4-CP in real water samples by the proposed sensor.

4-CP concentration (ng mL^{-1})				
sample	added	found	recovery	RSD
1	8.00	8.23	102. 87%	3.60%
2	80.00	82.19	102.73%	3.70%
3	400.00	397.00	99.25%	2.40%
4	1200.00	1193.20	99.41%	4.20%
5	2000.00	1987.00	99.35%	2.8%

References

1 D. Liu, W.B. Cai, Y.G. Wang and Y.F. Zhu, *Appl. Catal., B* 2018, **236**, 205-211.

2 Y.F. Liu, Y.H. Lv, Y.Y. Zhu, D. Liu, R.L. Zong and Y.F. Zhu, *Appl. Catal., B* 2014, **147**, 851-857.

3 Y.Y. Zhu, Y.F. Liu, Y.H. Lv, Q. Ling, D. Liu and Y.F. Zhu, *J. Mater. Chem. A* 2014, **2**, 13041-13048.

4 J. Di, J.X. Xia, S. Yin, H. Xu, M.Q. He, H.M. Li, L. Xu and Y.P. Jiang, *RSC Adv.* 2013, **3**, 19624-19631.

5 Z. Mo, H. Xu, Z.G. Chen, X.J. She, Y.H. Song, P.C. Yan, Y.G. Xu, Y.C. Lei, S.Q. Yuan and H.M. Li, *Chin. J. Catal.* 2018, **39**, 760-770.

6 L. Xu, J.X. Xia, L.G. Wang, J. Qian, H.M. Li, K. Wang, K.Y. Sun and M.Q. He, *Chem. Eur. J.* 2014, **20**, 2244-2253.

7 B. Wang, O.K. Okoth, K. Yan and J.D. Zhang, *Sens. Actuators, B* 2016, **236**, 294-303.

8 L. Wang, Q. Sun, Y. Liu and Z.S. Lu, *RSC Adv.* 2016, **6**, 34692-34698.

9 X.L. Zhu, K.X. Zhang, D.W. Wang, D.M. Zhang, X. Yuan and J. Qu, *J. Electroanal. Chem.* 2018, **810**, 199-206.

10 C.C. Qiu, T. Chen, X. Wang, Y. Li and H.Y. Ma, *Colloids Surf. B.* 2013, **103**, 129-135.